

Theoretical analysis of initial adsorption of high- κ metal oxides on $\text{In}_x\text{Ga}_{1-x}\text{As}(0\ 0\ 1)-(4\times 2)$ surfaces

Sarah R. Bishop, Jonathon B. Clemens, Evgueni A. Chagarov, Jian Shen,^{a)} and Andrew C. Kummel^{b)}

Department of Chemistry and Biochemistry, University of California, San Diego, 9500 Gilman Drive 0358, La Jolla, California 92093-0358, USA

(Received 8 January 2010; accepted 23 September 2010; published online 17 November 2010)

Ordered, low coverage to monolayer, high- κ oxide adsorption on group III rich $\text{InAs}(0\ 0\ 1)-(4\times 2)$ and $\text{In}_{0.53}\text{Ga}_{0.47}\text{As}(0\ 0\ 1)-(4\times 2)$ was modeled via density functional theory (DFT). Initial adsorption of HfO_2 and ZrO_2 was found to remove dangling bonds on the clean surface. At full monolayer coverage, the oxide-semiconductor bonds restore the substrate surface atoms to a more bulklike bonding structure via covalent bonding, with the potential for an unpinned interface. DFT models of ordered $\text{HfO}_2/\text{In}_{0.53}\text{Ga}_{0.47}\text{As}(0\ 0\ 1)-(4\times 2)$ show it fully unpins the Fermi level. © 2010 American Institute of Physics. [doi:10.1063/1.3501371]

I. INTRODUCTION

The future of III-V based metal-oxide-semiconductor (MOS)-type devices relies on the ability to form a passive interface between the gate oxide and the semiconductor. Native oxide formation on III-V materials contains defects at the oxide-semiconductor interface, creating trap states which degrade device performance.^{1,2} High- κ dielectrics which refer to a material with a high dielectric constant, a measure of the electric field induced by an oxide of a given thickness with a given applied potential, such as HfO_2 and ZrO_2 , are an attractive choice for a gate oxide material to maximize control of channel current while minimizing gate leakage current.^{3,4} A recent study of the interface between HfO_2 and $\text{In}_{0.53}\text{Ga}_{0.47}\text{As}$ for a MOS diode found that native oxide at the interface yields poor electronic properties compared to direct deposition of high- κ on the semiconductor.⁴

Direct oxidation can disrupt semiconductor substrates, possibly inducing new states in the Fermi level region. For example, O_2 dosing on $\text{InAs}(0\ 0\ 1)-(4\times 2)$ displaces the row-edge As atoms and creates excess As atoms;⁵ furthermore, O_2 dosing of $\text{Ge}(001)-(4\times 2)$ displaces surface Ge atoms and creates Ge adatoms.⁶ Two deposition methods that have found success in forming low defect density oxide-III/V interfaces are molecular beam deposition (MBE) and atomic layer deposition (ALD). The importance of the structure of the first oxide layer has been demonstrated for both MBE and ALD gate oxides deposition. For example, Hale *et al.* showed that the first layer of Ga_2O deposition is critical in unpinning the oxide/GaAs interface in low temperature MBE of $\text{GGO}/\text{Ga}_2\text{O}_3/\text{GaAs}(0\ 0\ 1)-(2\times 4)$ oxide stacks because the Ga_2O restores the surface to a more bulklike termination and maintains an unpinned interface to the oxide.^{7,8} ALD oxide growth offers greater control of the high- κ /semiconductor interface at low temperature ($\sim 200\text{--}320\text{ }^\circ\text{C}$), and limits the formation of arsenic

oxides;⁹⁻¹² the low temperature processing of ALD is consistent with the bonding and structure of the first layer being critical to having an unpinned interface in the complete oxide-semiconductor stack. For example, Clemens *et al.*¹³⁻¹⁵ shows that the first layer of TMA on $\text{InGaAs}(0\ 0\ 1)-(4\times 2)$ changes the surface reconstruction, unpins the Fermi level, and provides a monolayer nucleation density template.

The atomic structure of clean $\text{InAs}(0\ 0\ 1)-(4\times 2)$ and $\text{In}_{0.53}\text{Ga}_{0.47}\text{As}(0\ 0\ 1)-(4\times 2)$ was recently determined as consistent with the $\beta 3'(4\times 2)$ reconstruction through a combination of scanning tunneling microscopy (STM) and density functional theory (DFT).^{16,17} The group III-rich (4×2) reconstructions of InAs and $\text{In}_{0.53}\text{Ga}_{0.47}\text{As}$ surfaces are of particular interest as a starting reconstruction due to their low reactivity to oxygen in comparison to the As-rich (2×4) reconstructions.⁵ It has been reported that the $\text{InAs}(0\ 0\ 1)$ surface has an electron accumulation layer at the surface where the Fermi level resides within the conduction band.^{18,19} Robertson²⁰ proposed an interface states model for group III-V semiconductors in which surface defects such as dangling bonds or like-atom bonding states impact the Fermi level. The clean, $\beta 3'(4\times 2)$ surface is pinned by nonbulklike atoms on the surface. An unpinned interface is possible if the direct cause of pinning is attributed solely to surface states and surface defects, since they can be passivated by fortuitous adsorbate binding.

Clemens *et al.*²¹ experimentally found that deposition via e^- beam evaporation of HfO_2 at full coverage on $\text{In}_{0.53}\text{Ga}_{0.47}\text{As}(0\ 0\ 1)-(4\times 2)$ partially unpins the Fermi level compared to the clean $\beta 3(4\times 2)$ reconstruction. This was attributed to the covalent bond network between the oxide and semiconductor surface, consistent with the postannealing formation of ordered regions on the surface. It was suggested that while HfO_2 can passivate surface states created by the clean surface reconstruction, the incongruent nature of e^- beam evaporated HfO_2 allowed for oxidation and displacement of substrate atoms to occur thereby limiting the improvement in electronic structure. These results show

^{a)}Electronic mail: jimshen@ucsd.edu.

^{b)}Electronic mail: akummel@ucsd.edu.

promise for realization of an unpinned high- κ oxide/semiconductor interface with careful selection of processing conditions.

In the present study, the atomic and electronic structures of ordered HfO₂ and ZrO₂ adsorption sites as a function of coverage up to one monolayer on InAs(0 0 1)-(4×2) were modeled via DFT. The atomic structures of adsorbates were analyzed on the InAs(0 0 1)-(4×2) surface due to the simplicity of the atomic structure of InAs compared to InGaAs. The In_{0.53}Ga_{0.47}As(0 0 1)-(4×2) surface is analogous to that of InAs(0 0 1)-(4×2).¹⁷ However, the larger band gap of In_{0.53}Ga_{0.47}As(0 0 1)-(4×2) improves the ease of analysis of the electronic properties for both DFT simulation and scanning tunneling spectroscopy experiments.²¹ In this study, the electronic structure was determined for HfO₂ on In_{0.5}Ga_{0.5}As(0 0 1)-(4×2) along with a comparison between perfectly ordered and semiordered HfO₂ adsorption on the In_{0.5}Ga_{0.5}As(0 0 1)-(4×2) surface for comparison to the experimental results. DFT results found monolayer coverage of both HfO₂ and ZrO₂ restored the substrate surface atoms to near bulklike bonding, with potential to form an unpinned interface.

II. COMPUTATIONAL METHODS

DFT simulations were performed with the Vienna *ab initio* simulation package (VASP), a plane wave code with periodic boundary conditions, for both geometric and electronic structure calculations.^{22–25} Simulations were performed with the Perdew–Burke–Ernzerhof^{26,27} (PBE) exchange-correlated functional of the generalized gradient approximation using the projector augmented wave (PAW) pseudopotentials (PP) supplied with VASP.^{28,29}

2×4×1 Monkhorst–Pack *K*-point sampling was chosen based on analysis of total energy saturation for several calculated $N \times 2N \times 1$ (N -integer) Monkhorst–Pack grids.³⁰ For the 2×4×1 grid, the total energy of the slab approaches the saturation value and is close to the total energy calculated at 3×6×1 and 4×8×1 grids. The 2×4×1 grid was chosen due to higher computational efficiency required for DFT-molecular dynamics (MD) calculations. Besides energy, forces and electronic structure were calculated for several progressive *K*-point grids and did not reveal significant deviations in values between 2×4×1 and higher-order *K*-point grids. Therefore 2×4×1 Monkhorst–Pack sampling grid was employed in the present study.

The system geometry was relaxed by conjugate-gradient relaxation algorithm to have forces below a force tolerance level of 0.03 eV/Å. The choice of PBE functional and PAW PP was validated by parameterization runs comparing DFT-calculated bulk properties to experimental values. The PAW-PP for the In atom did not treat the 4*d* electrons in the valence state. A comparison test between In PPs that included the 4*d* electrons in the core or part of the valence was performed; the results showed little difference among the bonding energies, geometries, and resulting electronic structure.

The slab models were constructed based on DFT-optimized lattice constant value. The DFT lattice constants

for InAs and InGaAs were obtained by standard fitting of Murnaghan equation of state to the set of DFT calculated total energies at different unit cell volumes obtained by unit cell rescaling and relaxation. The lattice constant increment trial step was 0.1 Å. The unit cell relaxations did not produce any internal geometry changes due to high symmetry of InAs and InGaAs unit cells and therefore were equivalent to total energy calculations. This was done separately for InAs and InGaAs. The calculated lattice constant for InAs was 6.22 Å while the calculated lattice constant for In_{0.5}Ga_{0.5}As was 5.99 Å, which correlated well with the experimental values of 6.06 Å for InAs and 5.87 Å for In_{0.53}Ga_{0.47}As.³¹

The clean InAs(0 0 1)-(4×2) surface was modeled on a double slab, two (4×2) unit cells (~17.58×17.58 Å²) containing a total of 156 atoms, with periodic boundaries conditions. The slab consisted of eight layers of atoms (~12 Å) and a 19 Å vacuum layer with the bottom In atomic layer hydrogen-terminated with pseudohydrogen atoms containing a charge of 1.25 *e*⁻ to simulate bulklike properties.³² In addition, the bottom three layers of the InAs slab were frozen in the bulk position to preserve the bulklike properties of the slab.

A simulated slab of In_{0.5}Ga_{0.5}As(0 0 1)-(4×2) has recently been shown to reliably model experimental results of the clean In_{0.53}Ga_{0.47}As(0 0 1)-(4×2) surface.¹⁷ The clean In_{0.5}Ga_{0.5}As(0 0 1)-(4×2) surface was modeled on a double slab, two (4×2) unit cells (~16.95×16.95 Å²) containing a total of 140 atoms, with periodic boundary conditions. The slab consisted of seven atomic layers (~10 Å) and a ~12 Å vacuum layer. The three bottom InGaAs layers were permanently fixed in their bulklike positions. The systems with bottom As atoms were terminated by pseudohydrogen atoms with a charge of 0.75 *e*⁻. The utilized PAW pseudopotentials for In and Ga atoms treated In 4*d* and Ga 3*d* electrons as core electrons, which provided higher efficiency and faster electronic convergence at satisfactory computational accuracy.

In the present study, both DFT geometry optimization (below force tolerance level of 0.02 eV/Å) and MD (DFT-MD) calculations were performed in which two molecules of HfO₂ were deposited on a single slab of the In_{0.5}Ga_{0.5}As(0 0 1)-(4×2) surface. The initial, relaxed InGaAs slab configuration for both types of simulations was previously reported by Shen *et al.*,¹⁷ where an in depth description of the InGa alloying is described. DFT-MD simulated annealing and cooling the surface; therefore, atoms could diffuse prior to relaxation to the ground state structure. DFT-MD was used to simulate a semiordered adsorption structure of the HfO₂ molecules. The basic method for DFT-MD utilized in this study has been described elsewhere, but is briefly reviewed here.^{33,34} An initial structure of the bridge site, two HfO₂ molecules adsorbed on the In_{0.5}Ga_{0.5}As(0 0 1)-(4×2) surface, was annealed at 800 K for 1000 fs with 1.0 fs time step, cooled to 0 K for 200 fs, and relaxed below 0.02 eV/Å force tolerance level. The three bottom semiconductor layers were permanently frozen in their bulklike positions. A comparison of the ordered (produced by DFT geometry optimization) and semiordered (pro-

duced by DFT-MD) atomic and electronic structures at full coverage was evaluated for monolayer HfO_2 adsorption onto $\text{In}_{0.5}\text{Ga}_{0.5}\text{As}(0\ 0\ 1)-(4\times 2)$.

The binding energy (ΔE) was calculated for each binding site studied, and the relative error between binding energies for similar binding sites on the same substrate is assumed to be ± 0.1 eV using this method.³⁵ The absolute and relative method errors (exchange correlation functional, various approximations, atomic potential, etc.) are not straightforward to estimate. Absolute method errors quantify the agreement between the computational results and experimental data. The mean absolute error (absolute method error) with respect to experimental values of the G2-1 test set using VASP, with PAW pseudopotentials and PBE exchange-correlation functional was calculated by Paier *et al.*³⁶ as 0.37 eV. However, the relative method errors expected in the current study may be smaller. The relative method error is the uncertainty in the total energy difference between two similar adsorption sites. This has not been precisely calculated, but many DFT papers using similar techniques to the ones employed in the current manuscript papers report differences in binding energy at similar adsorption sites on the same surface of ± 0.10 eV to be significant.^{37,38}

III. RESULTS AND DISCUSSION

Treatment of semiconductor materials with standard DFT results in an underestimation of the band gap. This is due to the approximate nature of the exchange potential of the exchange-correlation functional.^{39,40} For bulk InAs , the band gap calculated by DFT with a PBE functional is metallic. Alternatively, $\text{In}_{0.5}\text{Ga}_{0.5}\text{As}$, with a greater band gap compared to $\text{InAs}(0\ 0\ 1)-(4\times 2)$, was calculated by DFT with PBE functional to be semiconducting, not metallic. Experimentally, these semiconductors are known to have band gaps of 0.35 eV for InAs and 0.74 eV for $\text{In}_{0.53}\text{Ga}_{0.47}\text{As}$.³¹ The DFT-calculated band gap can be artificially expanded by quantum confinement for nonbulk simulations. DFT simulations in this report have wider band gaps for InGaAs slabs than for InGaAs bulk due to quantum confinement in vertical direction due to limited slab thickness ($\sim 7-10$ Å). The DFT-calculated band gap for InGaAs bulk is ~ 0.4 eV while for the slab it is ~ 0.9 eV (supplementary Fig. 1).⁴¹ The slab band gap value was calculated with different K -point sampling and no significant band-gap variation was observed between the $2\times 4\times 1$ K -point grid and denser grids. (supplementary Fig. 1).⁴¹ One way to minimize quantum confinement in slab calculations is to increase slab thickness or slab size; however, at present, due to high computational cost of DFT and especially DFT-MD simulations, substantially increasing the slab size is computationally prohibitive since the current slab size already contains 156 atoms.

To determine the impact on the interfacial electronic properties of adsorption of an oxide molecule on the III-V semiconductor surface, this study relies on analysis of density of states (DOS) at the Fermi level region. An increase of density of states in the band gap region at the Fermi level suggests the introduction of possible pinning states in the band gap. If there is a decrease or no change in density of

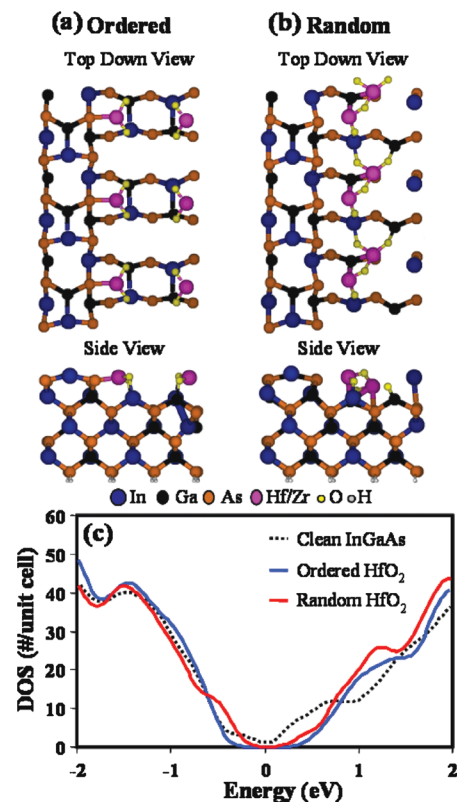


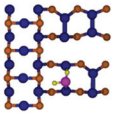
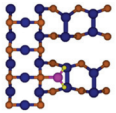
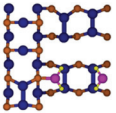
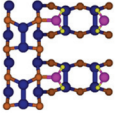
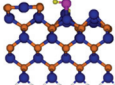
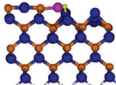
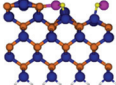
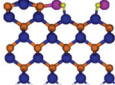
FIG. 1. DFT and DFT-MD calculated atomic and electronic structures of full coverage (a) ordered and (b) semiordered HfO_2 adsorption on a single unit cell $\text{In}_{0.5}\text{Ga}_{0.5}\text{As}(0\ 0\ 1)-(4\times 2)$ surface. The atomic structures are depicted via ball-and-stick diagrams denoted with In (blue), Ga (black), As (brown), Hf (magenta), O (yellow), and H (white) atoms. Both top down views (three repeating single unit cells produced with periodic boundary conditions to show the bonding network) and side views (full slab including terminating H atoms). (c) The DFT calculated total DOS for the ordered (blue) and semiordered (red) HfO_2 adsorbed surfaces compared to the clean, $\text{In}_{0.5}\text{Ga}_{0.5}\text{As}(0\ 0\ 1)-(4\times 4)$ (dashed black line). The DOS is the density of states per single unit cell for each structure. For all simulated DOS, the deep valence band states are aligned, and the Fermi level (E_F) is at 0.0 eV.

states in the band gap region, it is suggested that the adsorption site does not induce Fermi level pinning.

A. Clean $\text{InAs}(0\ 0\ 1)-(4\times 2)$ and $\text{InGaAs}(0\ 0\ 1)-(4\times 2)$

The clean atomic structures for both $\text{InAs}(0\ 0\ 1)-(4\times 2)$ (Ref. 16) and $\text{In}_{0.53}\text{Ga}_{0.47}\text{As}(0\ 0\ 1)-(4\times 2)$ (Ref. 17) were modeled previously with a combination of experiment and theory based techniques: STM and DFT. The STM and DFT studies found the atomic structures for both InAs and InGaAs to be analogous. The clean group III-rich (4×2) reconstruction consists of single, dicoordinated undimerized row In/Ga atoms in the $[1\ 1\ 0]$ direction bonded to row edge As in a sp -like bonding configuration, consisting of a flat, 179° $\text{As}-\text{In}/\text{Ga}-\text{As}$ bond angle. DFT-molecular dynamic (DFT-MD) simulations at elevated temperature show that the 300 K surface is a thermal superposition of three unbuckled reconstructions. However, the slow experimental STM imaging does not isolate the different reconstruction so the surface appear to be the lowest symmetry structure which is the $\beta 3'(4\times 2)$.¹⁷ Determination of the atomic structure of both the clean and adsorbate-covered surface is simpler for

TABLE I. Summary of the computational results for ordered MO_2 ($M=\text{Hf, Zr}$) adsorption on $\text{InAs}(0\ 0\ 1)\text{-(}4\times 2\text{)}$ as a function of coverage up to one monolayer. Results include calculated binding energies (eV) for both hafnium and zirconium oxide, and the top down and side view of the double slab structure for the four MO_2 adsorption sites identified (trough, row edge, bridge, and full coverage) where the final structures for each site were identical for both oxides.

	Trough	Row Edge	Bridge	Full Coverage
$E_{\text{bind}}(\text{HfO}_2)^a$	-2.76 eV	-3.95 eV	-4.34 eV	-4.29 eV
$E_{\text{bind}}(\text{ZrO}_2)^a$	-2.22 eV	-3.45 eV	-3.82 eV	-3.78 eV
Top down view				
Side View				

^a Calculated binding energies, E_{bind} are given with respect to the clean double unit cell $\text{InAs}(0\ 0\ 1)\text{-(}4\times 2\text{)}$ surface and a single MO_2 molecule

● In ● As ● Hf/Zr
○ O ○ H

InAs in comparison to InGaAs due to the lower surface defect density along with unambiguous assignment of the group III atoms as In. Additionally, the lack of the experimental trough charge density features simplifies the MO_2 bonding geometry determination on InAs . Therefore atomic structure models are focused on high- κ adsorption on $\text{InAs}(0\ 0\ 1)\text{-(}4\times 2\text{)}$.

B. High- κ oxide adsorption on $\text{InAs}(0\ 0\ 1)\text{-(}4\times 2\text{)}$

Simulations of HfO_2 and ZrO_2 ordered adsorption as a function of coverage were performed and binding energies, atomic structures, and electronic structures are reported. The adsorption sites modeled were chosen specifically to resemble the results of an experimental STM study of HfO_2 adsorption on $\text{InAs}(0\ 0\ 1)\text{-(}4\times 2\text{)}$ performed by Clemens *et al.*²¹ At low coverage, STM studies show that HfO_2 molecules preferentially bind in the trough, adjacent to the As row edge, in comparison to molecular adsorption on the row. In addition, HfO_2 formed bridge sites in which two HfO_2 molecules spanned the trough, binding to the edges of opposing rows. This is consistent with an attractive interaction between pairs of HfO_2 adsorbates.

Table I contains four ball-and-stick diagrams of the relaxed MO_2 adsorption structures and their corresponding binding energies. Both top down and side view ball-and-stick diagrams for the four sites simulated are presented in Table I, where the side view shows the entire slab thickness including the pseudohydrogen termination layer. It was found that HfO_2 and ZrO_2 bond identically to the surface. All adsorption geometries presented in Table I can be applied to either Hf or Zr as the metal (M) in the MO_2 molecules. The major difference between the two high- κ materials is the binding energy for each site. The “binding energies” were calculated by subtracting the total energy of the most stable clean surface structure and gas phase oxide molecule from the total energy of the oxide/ InAs complex. These are “binding energies” as defined by Lee *et al.*⁴² because the energy of the adsorbate complex is compared to that of the clean surface and the gas phase adsorbate instead of a true bulk reference

state for the adsorbate. The binding energies for ZrO_2 are ~ 0.5 eV less exothermic per molecule compared to the identical HfO_2 adsorption sites. Similar binding energies were obtained for the DFT simulated ordered monolayer MO_2 on the $\text{Ge}(0\ 0\ 1)\text{-(}4\times 2\text{)}$ substrate as well.⁴³

The first two simulations are two single MO_2 adsorption sites near or on the row edge. The trough single insertion site, identified as the trough site in this paper, is energetically stable with a $E_{\text{bind}}(\text{HfO}_2)=-2.76$ eV and $E_{\text{bind}}(\text{ZrO}_2)=-2.22$ eV. As shown in the ball-and-stick diagrams of the relaxed trough site (both top down and side views), the M atom forms a $M\text{-In}$ bond and maintains bonds to both oxygen atoms. One of the oxygen atoms bonds to the other available In dimer atom, while the second oxygen maintains a double bond to the M atom.

The row edge single insertion site (Table I) has a lower total energy (i.e., greater binding energy at 0 K) compared to the trough single insertion site, $E_{\text{bind}}(\text{HfO}_2)=-3.95$ eV and $E_{\text{bind}}(\text{ZrO}_2)=-3.45$ eV. The metal atom bonds to the almost filled dangling bond of the row edge As atom, and the oxygen atoms bond to the mostly empty dangling bonds of the trough In atoms of the dimer adjacent to the row edge creating a covalent bonding configuration. While a binding energy of -4 eV would be considered a strong, ionic bond for a single atom, the MO_2 molecule forms three new bonds to the surface, each of which is a weak polar covalent bond. For both single insertion sites, In dimer buckling occurs on two trough In dimers in both the $[1\ 1\ 0]$ and $[-1\ 1\ 0]$ directions adjacent to the adsorption site. While the row edge site more closely resembles the single insertion sites in the experimental STM study, there is no experimental evidence of trough dimer buckling.²¹

The other common site found experimentally at low coverage is the bridge site. The simulated bridge site for MO_2 molecules, as shown in Table I, comprises of two opposing row edge sites that span the trough. The bridge site is energetically favored by ~ 0.4 eV per MO_2 compared to the single row edge site, supporting the total energy drive to form bridge sites, consistent with experiments. By forming a bridge site in the trough region, the InAs surface dangling bonds at the trough and row edge are passivated by oxide adsorption, thereby preventing the formation of buckled In trough dimers bonded to MO_2 . However, one of the adjacent trough indium dimers does buckle.

In the bridge site, as well as the previously described row edge site, the M atom only forms a new bond to the row edge As while the O atoms form new bonds to the In trough dimer atoms. In comparison to the single row edge site, where the major adsorbate induced changes occur in the trough, the major adsorbate induced changes of the surface structure due to the formation of the bridge site occur both in the trough and on the row. The bridge site induces the two row In atoms adjacent to the As-M bond to form a dimer, where previously the row was entirely undimerized. On the double unit cell slab, the bridge site corresponds to 50% coverage.

Ordered, full coverage MO_2 was modeled on the double unit cell slab (Table I). This site bonds in an identical way to the surface as the bridge site. As the coverage increases from

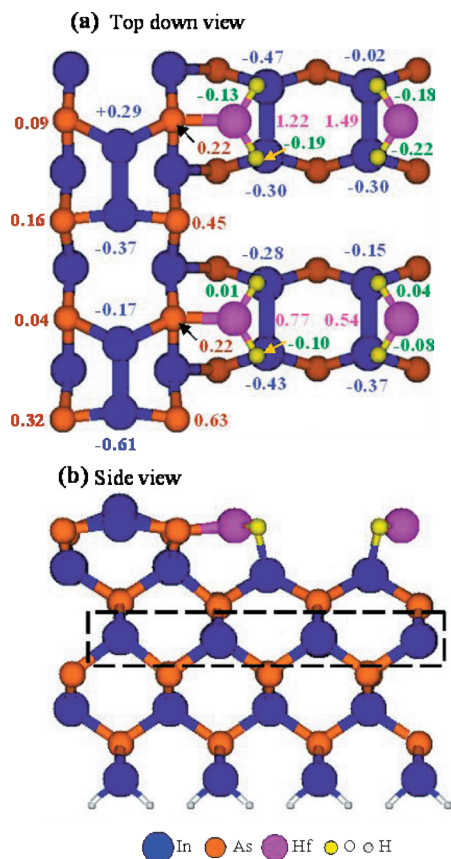


FIG. 2. Surface Bader charge analysis comparing the atomic charges of full coverage $HfO_2/InAs(0\ 0\ 1)-(4\times 2)$ to the bulk InAs and gas phase HfO_2 . A top down view (a) with the charge difference, $|e|$, for In (blue), As (brown), Hf (magenta), and O (green) listed next to the respective atoms. The loss of electron density is indicated by the (-) sign. A side view (b) shows the fourth layer In atoms (shown in dashed box) which have an increased atomic charge compared to bulk In atomic charge, on average.

50% to 100%, the row In atoms become entirely dimerized and the trough does not form any buckled trough dimers. The binding energy for the full coverage site is -4.29 eV per HfO_2 and -3.78 eV per ZrO_2 , ~ 0.05 eV less exothermic than the bridge site for both MO_2 molecules. Within the limitation of the DFT method employed, 50% and 100% coverages are energetically degenerate. Both 50% and 100% coverages form via weak polar covalent bonds to the surface, with the total binding energy representing three bonds to the substrate. The electronic structures for the four HfO_2 and ZrO_2 sites described in this section (trough insertion, row edge site, bridge site, and full coverage) are also calculated and shown in supplementary Figs. 2(a)–2(d).⁴¹

C. $HfO_2/In_{0.5}Ga_{0.5}As(0\ 0\ 1)-(4\times 2)$

A limitation of the simulated electronic structure results on $InAs(0\ 0\ 1)-(4\times 2)$ slab is the difficulty in discerning between true states in the band-gap region and overlap of the valence and conduction band edges. Fortunately, the $In_{0.53}Ga_{0.47}As(0\ 0\ 1)-(4\times 2)$ reconstruction has been shown to be structurally analogous to the $InAs(0\ 0\ 1)-(4\times 2)$ reconstruction but with an increase in the band gap, as shown in both STM and DFT.¹⁷ Shen *et al.* also found that the

specific placement of the group III atoms, Ga and In, does not impact electronic structure of the clean slab.

To confirm the interpretation of MO_2 adsorption on InAs results, a simulation of full coverage HfO_2 on a single unit cell slab $In_{0.5}Ga_{0.5}As(0\ 0\ 1)-(4\times 2)$ was performed. The relaxed, final geometry resulted in a bridge site and is shown on a triple slab in Fig. 1(a) (three repeating single unit cells, depicted via periodic bonding configurations); the bonding structure is identical to the HfO_2 bridge site on $InAs(0\ 0\ 1)-(4\times 2)$ with In (blue), Ga (black), As (brown), Hf (magenta), O (yellow), and H (white) atoms (color). The bonding configuration produces only Hf–As bonds and In/Ga–O bonds, where the metal atom bonds to the almost filled dangling bond of the As and the O atoms bond to the mostly empty dangling bonds of the In trough atoms.

The electronic structure for the single slab calculation of the ordered adsorption of HfO_2 on $In_{0.5}Ga_{0.5}As(0\ 0\ 1)-(4\times 2)$ compared to the simulated low temperature clean structure, $(\beta 3')(4\times 4)$, is shown in Fig. 1(c). A double slab is necessary to relax the $\beta 3'(4\times 4)$ surface compared to $\beta 3'(4\times 2)$; therefore, the DOS for $\beta 3'(4\times 4)$ is normalized to a single unit cell. There is no additional density of states in the Fermi level region postadsorption of HfO_2 on the surface, but more striking is the reduction of states at both the valence and conduction band edges occurs, creating an improved band gap. This strongly suggests for both $In_{0.5}Ga_{0.5}As$ and InAs surfaces, an ordered MO_2 interface may unpin the surface with ideal processing conditions.

A second simulation was performed on $In_{0.5}Ga_{0.5}As$ to simulate possible effects including semioorder of an annealed surface interface with the high- κ dielectric on the electronic structure. To simulate annealed full coverage HfO_2 adsorption sites, DFT-MD was employed. Two HfO_2 molecules were bonded in the bridge configuration on a single unit cell slab of the $In_{0.5}Ga_{0.5}As$ surface, followed by a simulated annealing at 800 K, cooling, and final relaxation. The resulting relaxed structure, which created a semioordered interface, is depicted in Fig. 1(b) with three repeating single units produced via periodic boundary conditions. While the majority of MO_2 bonds to the surface occur through the predicted M–As and O–In/Ga pathways, one M–In/Ga bond exists, per unit cell, similar to the single trough site simulated for the InAs surface (Table I). In addition, a group III atom, trough In, is displaced from the substrate only forming one bond to a trough As.

The semioordered bonding scheme on the electronic structure is depicted in Fig. 1(c), with the resultant band gap for the $HfO_2/In_{0.5}Ga_{0.5}As$ surface impacted by the alternative bonding structure. The electronic structure of the DFT-MD annealed structure [Fig. 1(b)] compared to the ordered HfO_2 overlayer [Fig. 1(a)] electronic structure is not as improved, lacking the widening of the band gap. However, the DOS for the semioordered bonding scheme shows an improvement compared to the DOS of the clean reconstruction. These results are consistent with the scanning tunneling spectroscopy (STS) data of Clemens *et al.* showing a partial unpinning of the Fermi level for e -beam deposited HfO_2 on $In_{0.53}Ga_{0.47}As(0\ 0\ 1)-(4\times 2)$ with partial oxide disorder.

IV. BADER CHARGE ANALYSIS

To determine the nature of the MO_2 bond to the semiconductor surface through theoretical methods, a Bader analysis of surface charge transfer was performed.^{44–46} A comparison of charge between the adsorbed surface and bulk In and As is presented in Fig. 2, for the ordered full coverage $HfO_2/InAs$ site. The bulk In and As atom Bader charges were subtracted from the total charge for each In and As atom in the double unit cell, respectively. Compared to the bulk In and As charges, most surface atoms directly bonded to the HfO_2 molecules, row edge As, and trough dimer In atoms, contain small charge differences, with a mean charge difference of $\pm 0.25 |e|$ ($|e|$ = electron). Only four atoms on the surface contain a charge difference greater than $\pm 0.5 |e|$ between the bulk In or As charge. These results are qualitatively consistent with experimental x-ray photoelectron spectroscopy (XPS) data for HfO_2 on group III rich III–V surface.⁴⁷

A Bader analysis was also employed to determine the full coverage oxide induced charge transfer to the semiconductor surface atoms relative to the clean surface $\beta 3'(4 \times 2)$ reconstruction. The oxide bonded surface In atoms had an average loss of $-0.26 |e|$ while the surface As atoms had an average gain of $+0.15 |e|$ compared to the clean surface. The clean $\beta 3'(4 \times 2)$ reconstruction contains an abnormal charge on two surface In atoms, in the second layer on the row ($-1.5 |e|$ compared to bulk In atoms), which were not included in the above average charge transfer calculation. However, oxide bonding also restores these two charged In atoms to bulklike charge.

Furthermore, the $HfO_2/InAs$ structure contained non-bulklike charge on 50% of the atoms in the fourth layer which is unchanged by oxide bonding. This suggests the nonbulklike charge is not a result of oxide adsorption alone. The charge transfer relative to the clean surface is consistent with the HfO_2 adsorption to the surface occurs via polar covalent bonding, which would give a near zero chemical shift in XPS and is consistent with experimental results.¹⁰ Experimental XPS results found HfO_2 films grown via ALD on $In_{0.53}Ga_{0.47}As$ or $GaAs$ produced very minimal chemical shifts at the interface and no As–O bonds, suggesting the semiconductor atoms are bulklike due to the polar covalent nature of the oxide-semiconductor bonds.^{10,47,48}

V. CONCLUSION

DFT was utilized to determine the structural and electronic properties of the $HfO_2/$ and $ZrO_2/III-V$ monolayer and submonolayer interfaces. Four ordered MO_2 adsorption sites were simulated on both the clean $InAs(0\ 0\ 1)-(4 \times 2)$ and $In_{0.5}Ga_{0.5}As(0\ 0\ 1)-(4 \times 2)$ surfaces: trough site, row edge site, bridge site, and full coverage. The lowest energy MO_2 bonding configuration passivates the trough surface states occurs through M bonds to the almost filled dangling bonds of the row edge As and O bonds to the mostly empty dangling bonds of the trough In/Ga dimer atoms. The MO_2 molecule forms polar covalent bonds to the surface. The adsorption of MO_2 to the substrate restores the surface atoms to more bulklike sp^3 tetrahedral bonding structures. The elec-

tronic property results for monolayer HfO_2 and ZrO_2 strongly support the potential of the formation of an unpinned interface.

ACKNOWLEDGMENTS

This work was supported through the SRC Nonclassical CMOS Research Center (task ID 1437.003) and NSF-DMR (task ID 0706243), and the FCRP-MSD (task ID 887.011) grants. Sarah Bishop would like to thank the GRC and GLOBALFOUNDRIES for a sponsored GRC Graduate Fellowship for support.

- ¹M. L. Huang, Y. C. Chang, C. H. Chang, Y. J. Lee, P. Chang, J. Kwo, T. B. Wu, and M. Hong, *Appl. Phys. Lett.* **87**, 252104 (2005).
- ²W. E. Spicer, P. W. Chye, P. R. Skeath, C. Y. Su, and I. Lindau, *J. Vac. Sci. Technol.* **16**, 1422 (1979).
- ³R. Engel-Herbert, Y. Hwang, J. Cagnon, and S. Stemmer, *Appl. Phys. Lett.* **95**, 062908 (2009).
- ⁴K. Y. Lee, Y. J. Lee, P. Chang, M. L. Huang, Y. C. Chang, M. Hong, and J. Kwo, *Appl. Phys. Lett.* **92**, 252908 (2008).
- ⁵J. B. Clemens, S. R. Bishop, D. L. Feldwinn, R. Droopad, and A. C. Kummel, *Surf. Sci.* **603**, 2230 (2009).
- ⁶T. J. Grassman, S. R. Bishop, and A. C. Kummel, *Surf. Sci.* **602**, 2373 (2008).
- ⁷M. J. Hale, S. I. Yi, J. Z. Sexton, A. C. Kummel, and M. Passlack, *J. Chem. Phys.* **119**, 6719 (2003).
- ⁸M. Passlack, J. K. Abrokwhah, R. Droopad, Z. Y. Yu, C. Overgaard, S. I. Yi, M. Hale, J. Sexton, and A. C. Kummel, *IEEE Electron Device Lett.* **23**, 508 (2002).
- ⁹C. H. Chang, Y. K. Chiou, Y. C. Chang, K. Y. Lee, T. D. Lin, T. B. Wu, M. Hong, and J. Kwo, *Appl. Phys. Lett.* **89**, 242911 (2006).
- ¹⁰Y. C. Chang, M. L. Huang, K. Y. Lee, Y. J. Lee, T. D. Lin, M. Hong, J. Kwo, T. S. Lay, C. C. Liao, and K. Y. Cheng, *Appl. Phys. Lett.* **92**, 072901 (2008).
- ¹¹S. Koveshnikov, N. Goel, P. Majhi, H. Wen, M. B. Santos, S. Oktyabrsky, V. Tokranov, R. Kambhampati, R. Moore, F. Zhu, J. Lee, and W. Tsai, *Appl. Phys. Lett.* **92**, 222904 (2008).
- ¹²D. Wheeler, L. E. Wernersson, L. Fröberg, C. Thelander, A. Mikkelsen, K. J. Weststrate, A. Sonnet, E. M. Vogel, and A. Seabaugh, *Microelectron. Eng.* **86**, 1561 (2009).
- ¹³B. Shin, J. B. Clemens, M. A. Kelly, A. C. Kummel, and P. C. McIntyre, *Appl. Phys. Lett.* **96**, 252907 (2010).
- ¹⁴J. B. Clemens, E. A. Chagarov, M. Holland, R. Droopad, J. Shen, and A. C. Kummel, *J. Chem. Phys.* **133**, 154704 (2010).
- ¹⁵E. J. Kim, E. Chagarov, J. Cagnon, Y. Yuan, A. C. Kummel, P. M. Asbeck, S. Stemmer, K. C. Saraswat, and P. C. McIntyre, *J. Appl. Phys.* **106**, 124508 (2009).
- ¹⁶D. L. Feldwinn, J. B. Clemens, J. Shen, S. R. Bishop, T. J. Grassman, A. C. Kummel, R. Droopad, and M. Passlack, *Surf. Sci.* **603**, 3321 (2009).
- ¹⁷J. Shen, J. B. Clemens, E. A. Chagarov, D. L. Feldwinn, W. Melitz, T. Song, S. R. Bishop, R. Droopad, and A. C. Kummel, *Surf. Sci.* **604**, 1757 (2010).
- ¹⁸P. De Padova, C. Quaresima, P. Perfetti, R. Larciprete, R. Brochier, C. Richter, V. Ilakovac, P. Bencok, C. Teodorescu, V. Y. Aristov, R. L. Johnson, and K. Hricovini, *Surf. Sci.* **482**, 587 (2001).
- ¹⁹L. O. Olsson, C. B. M. Andersson, M. C. Hakansson, J. Kanski, L. Ilver, and U. O. Karlsson, *Phys. Rev. Lett.* **76**, 3626 (1996).
- ²⁰J. Robertson, *Appl. Phys. Lett.* **94**, 152104 (2009).
- ²¹J. B. Clemens, S. R. Bishop, J. S. Lee, A. C. Kummel, and R. Droopad, *J. Chem. Phys.* **132**, 244701 (2010).
- ²²G. Kresse, Technische University at Wien, 1993.
- ²³G. Kresse and J. Furthmüller, *Comput. Mater. Sci.* **6**, 15 (1996).
- ²⁴G. Kresse and J. Furthmüller, *Phys. Rev. B* **54**, 11169 (1996).
- ²⁵G. Kresse and J. Hafner, *Phys. Rev. B* **47**, 558 (1993).
- ²⁶J. P. Perdew, K. Burke, and M. Ernzerhof, *Phys. Rev. Lett.* **77**, 3865 (1996).
- ²⁷J. P. Perdew, K. Burke, and M. Ernzerhof, *Phys. Rev. Lett.* **78**, 1396 (1997).
- ²⁸P. E. Blochl, *Phys. Rev. B* **50**, 17953 (1994).
- ²⁹G. Kresse and D. Joubert, *Phys. Rev. B* **59**, 1758 (1999).
- ³⁰H. J. Monkhorst and J. D. Pack, *Phys. Rev. B* **13**, 5188 (1976).

- ³¹ See <http://www.ioffe.ru/SVA/NSM/> for semiconductor materials' characteristics and properties.
- ³² K. Shiraishi, *J. Phys. Soc. Jpn.* **59**, 3455 (1990).
- ³³ E. A. Chagarov and A. C. Kummel, *Surf. Sci.* **602**, L74 (2008).
- ³⁴ E. A. Chagarov and A. C. Kummel, *J. Chem. Phys.* **130**, 124717 (2009).
- ³⁵ D. L. Winn, M. J. Hale, T. J. Grassman, A. C. Kummel, R. Droopad, and M. Passlack, *J. Chem. Phys.* **126**, 084703 (2007).
- ³⁶ J. Paier, R. Hirschl, M. Marsman, and G. Kresse, *J. Chem. Phys.* **122**, 234102 (2005).
- ³⁷ N. Lorente, M. F. G. Hedouin, R. E. Palmer, and M. Persson, *Phys. Rev. B* **68**, 155401 (2003).
- ³⁸ S. E. Kul'kova, S. V. Eremeev, A. V. Postnikov, and I. R. Shein, *J. Exp. Theor. Phys.* **104**, 590 (2007).
- ³⁹ J. P. Perdew and M. Levy, *Phys. Rev. Lett.* **51**, 1884 (1983).
- ⁴⁰ L. J. Sham and M. Schlüter, *Phys. Rev. Lett.* **51**, 1888 (1983).
- ⁴¹ See supplementary material at <http://dx.doi.org/10.1063/1.3501371> for quantum confinement and K -point sample effects and DOS of MO_2 sites on InAs(0 0 1)-(4×2).
- ⁴² S. M. Lee, S. H. Lee, and M. Scheffler, *Phys. Rev. B* **69**, 125317 (2004).
- ⁴³ T. J. Grassman, S. R. Bishop, and A. C. Kummel, *Microelectron. Eng.* **86**, 249 (2009).
- ⁴⁴ G. Henkelman, A. Arnaldsson, and H. Jonsson, *Comput. Mater. Sci.* **36**, 354 (2006).
- ⁴⁵ E. Sanville, S. D. Kenny, R. Smith, and G. Henkelman, *J. Comput. Chem.* **28**, 899 (2007).
- ⁴⁶ W. Tang, E. Sanville, and G. Henkelman, *J. Phys.: Condens. Matter* **21**, 084204 (2009).
- ⁴⁷ T. Yasuda, N. Miyata, and A. Ohtake, *Appl. Surf. Sci.* **254**, 7565 (2008).
- ⁴⁸ C. L. Hinkle, A. M. Sonnet, E. M. Vogel, S. McDonnell, G. J. Hughes, M. Milojevic, B. Lee, F. S. Aguirre-Tostado, K. J. Choi, H. C. Kim, J. Kim, and R. M. Wallace, *Appl. Phys. Lett.* **92**, 071901 (2008).